

A TWO-PHASE MODEL FOR THE X-RAY EMISSION FROM SEYFERT GALAXIES

F. HAARDT AND L. MARASCHI

Dipartimento di Fisica, Università di Milano, via Celoria 16, 20133 Milano, Italy

Received 1991 July 2; accepted 1991 August 1

ABSTRACT

A two-phase accretion disk model is considered. A substantial fraction, f , of the gravitational power is assumed to be dissipated via buoyancy and reconnection of magnetic fields in a hot tenuous “corona” surrounding the main body of the disk. The main cooling mechanism of the hot layer is Comptonization of soft photons, thermally produced in the underlying cold phase. Hard Comptonized photons are backscattered into the thick phase, where they are in part reprocessed into the soft blackbody power and in part reflected. Coupled thermal balance equations for the two phases yield the temperature of the hot phase and the slope of the Comptonized component self-consistently as a function of f and τ , the optical depth of the hot phase. We find that for $f \simeq 1$, and $\tau < 1$, the temperature of the hot phase adjusts so as to maintain $\alpha \simeq 1$. For small τ the temperature of the hot phase is sufficient for production of electron-positron pairs to be important. Pair production contributes to the optical depth and limits the maximum temperature allowed. Monte Carlo simulations with parameters satisfying the balance equations show that, due to the asymmetry between forward and backward scattering, the transmitted spectrum in the 2–30 keV range is significantly flatter than derived from angle averaged formulae and the photon flux available for reprocessing in the thick layer is larger than 50%. The model accounts in a self-consistent way for the average power-law index and reflection component observed in the X-ray emission of Seyfert galaxies.

Subject headings: galaxies: nuclei — X-rays: spectra

1. INTRODUCTION

The X-ray spectra of Seyfert galaxies in the 1–10 keV range are remarkably uniform. Results from the *HEAO 1* and *EXOSAT* missions could be well described by single power laws, with a small spread in spectral indices, $\langle \alpha \rangle = 0.7 \pm 0.15$ (Rothschild et al. 1983; Mushotzky 1984; Turner & Pounds 1989). More recently, observations with the Japanese satellite *Ginga* clearly revealed the signature of “cold matter,” as envisaged by Guilbert & Rees (1988) and Lightman & White (1988), in the form of an Fe emission line and a broad hump around 10 keV, superposed on the power-law continuum, whose revised intrinsic slope is now estimated ~ 0.9 (Pounds et al. 1990). At least part of the cold matter should be located close to the X-ray production region, as indicated by the small time delays between the line and continuum variability (Kunieda et al. 1990). A natural site for it would be an accretion disk, whose thermal optically thick emission may account for the UV and/or soft X-ray excesses observed in these objects.

The origin of the “primary” power-law continuum is still unclear. A model extensively studied in the last years involves an injection mechanism of very high energy particles or photons (100–1000 MeV) initiating electron positron pair cascades, which in turn reprocess the primary spectrum via Compton scattering. This model has been found to be consistent with the observations, if reprocessing by cold matter is taken into account (Zdziarski et al. 1990, and references therein). Its main appeal is that pair reprocessing leads to a “canonical” spectrum largely independent of the details of the injection process and depending on only one source parameter, usually called compactness.

An alternative possibility, widely discussed in the 1970s, is that the power-law continuum is due to unsaturated Comptonization of soft photons by hot thermal electrons (Shapiro, Lightman, & Eardley 1976; Katz 1976; Pozdniakov,

Sobol, & Sunyaev 1976; Sunyaev & Titarchuk 1980). In this mechanism the resulting photon spectrum depends on the optical depth and temperature of the hot gas; therefore, any spectral shape can be reproduced with an ad hoc choice of these parameters. However, if the cooling of the hot gas is dominated by Comptonization, its temperature can be determined from a thermal balance equation. Models of this kind were developed using cyclosynchrotron photons in a hot accretion flow as the input for Comptonization (Takahara, Tsuruta, & Ichimaru 1981; Maraschi, Roasio, & Treves 1982).

Here we wish to reconsider thermal Comptonization as the basic mechanism for producing the X-ray power-law continuum of Seyfert galaxies in the framework of the new picture for the inner emission region. We assume that the release of gravitational power occurs in a hot optically thin region above a cooler optically thick layer, representing the usual accretion disk. The coexistence of the two phases is possible if the binding energy is dissipated outside the cool phase, as discussed by Begelman & de Kool (1990). A situation of this kind is envisaged in models of accretion disks with magnetic viscosity, in which dissipation occurs mainly through buoyancy and field reconnection in a magnetic corona above the disk (e.g., Burm 1986; Hayvaerts 1990 and references therein).

The main progress of the present model is that the two “phases” are coupled, i.e., the optically thick emission of the cool layer provides the soft photon input for Comptonization and the hard Comptonized photons contributed to the heating of the thick phase. The feedback between the two phases determines the fraction of the total power emitted in the three main spectral components, a blackbody from the optically thick phase, a power law from Comptonization in the hot layer, and a reflection component. We find that the resulting spectrum is largely independent of the coronal parameters and in agreement with the observations.

2. ENERGY BALANCE EQUATIONS FOR THE TWO PHASES

We approximate the two-phase disk as two uniform adjacent slabs. A fraction f of the gravitational power P_G is assumed to be dissipated in the hot layer, of optical depth to electron scattering τ , while $(1-f)P_G$ is the power dissipated within the optically thick phase. The hot phase is assumed to be tenuous, ($\tau < 1$), so that the main cooling mechanism is Comptonization of the soft photons emitted by the thick phase.

The total luminosity radiated in all directions by the hot phase (phase 2) can be expressed as AL_s , where A is the amplification factor due to Comptonization and L_s is the total soft photon luminosity emerging from the cool phase (phase 1). The luminosity added by the Compton process is $L_C = (A-1)L_s$. The Compton luminosity L_C can be broken down into the upward and downward components $L_C = L_{uc} + L_{dc}$, with $L_{dc} = \eta L_C$.

Hard photons directed downward are partly absorbed and partly reflected by the optically thick layer (Lightman & White 1988 and Guilbert & Rees 1988). The reflected power, $L_{rf1} = aL_{dc}$, will contribute to the hard component of the emitted spectrum, while the absorbed one, $(1-a)L_{dc}$, will contribute to L_s . Second-order reflection from the hot layer can be shown to be unimportant for $\tau < 1$.

The above considerations can be summarized in the following two equations:

Energy balance for phase 1:

$$(1-f)P_G + (1-a)L_{dc} = L_s \quad (1)$$

Energy balance for phase 2:

$$fP_G + L_s = AL_s \quad (2)$$

Solving for L_s and A , using the previous definitions, yields

$$L_s = \{1 - f[1 - (1-a)\eta]\}P_G \quad (3a)$$

$$A = 1 + \frac{f}{1 - f[1 - (1-a)\eta]} \quad (3b)$$

The outgoing luminosity L_{out} is given by

$$L_{out} = L_s + L_{uc} + L_{rf1} \quad (4)$$

with

$$L_{uc} = \frac{(1-\eta)f}{1-f+f\eta-fa\eta} L_s \quad (5a)$$

$$L_{rf1} = \frac{anf}{1-f+f\eta-fa\eta} L_s \quad (5b)$$

Clearly $L_{out} = P_G$. For small f the Comptonized and reflected component are proportional to fL_s , but if the limit $f=1$ they are determined solely by the values of η and a , which, for the relevant physical conditions, are between 0.5–0.6 and 0.1–0.2, respectively, as verified by Monte Carlo simulations (§ 4).

The energy balance equations (eqs. [3a] and [3b]) determine the value of the amplification factor A required in the Comptonization process. This in turn implies a relation between the optical depth and the temperature and therefore the spectral shape of the Comptonized component. In the case of $\tau < 1$ one can approximate the Comptonized spectrum with a power law (cf. Pozdnyakov et al. 1976; Rybicki & Lightman 1979)

$$I(\epsilon) = I(\epsilon_0) \left(\frac{\epsilon}{\epsilon_0} \right)^{-\alpha} \quad (6)$$

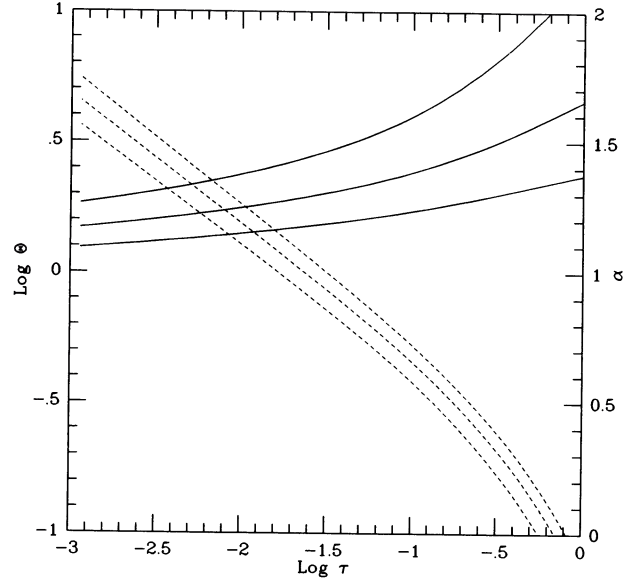


FIG. 1.—Electron temperature (dotted line, left scale) and average X-ray spectral index (solid line, right scale) as functions of the total optical depth τ . Higher $\Theta \equiv kT_C/m_e c^2$ and lower α correspond to increasing values of f . Different curves refer to $f = 0.5, 0.75, 1$.

where ϵ_0 is the average energy of the soft photons and $\alpha = -\ln \tau / \ln A_1$, where A_1 is the average energy gain in a single scattering. Thus, assuming $L_s \simeq I(\epsilon_0)\epsilon_0$, we can derive the following equation for the amplification in terms of the temperature T_C of the Comptonizing gas and the spectral index of the Comptonized component:

$$A - 1 = (1 - \alpha)^{-1} \left[\left(\frac{3kT_C}{\epsilon_0} \right)^{1-\alpha} - \left(\frac{\epsilon_1}{\epsilon_0} \right)^{1-\alpha} \right] \quad (7)$$

where $\epsilon_1 = A_1 \epsilon_0$.

We solve equation (7) by an iterative procedure using an expression for A_1 , valid at relativistic and subrelativistic temperatures, obtained from polynomial fitting of Monte Carlo simulations and checked with the results of Podznyakov, Sobol, & Sunyaev (1983). The derived values of α and T_C are plotted versus τ for various values of f in Figure 1.

The most important result apparent from Figure 1 is that, for a range of three orders of magnitude in τ , the spectral index α varies between 1.4 and 1.1 (for $f=1$). Thus the spectral shape is insensitive to the optical depth parameter. The physical reason is that the temperature adjusts so as to keep α nearly constant, as required for satisfying the energy balance equations.

The second result evident from the figure is that α is always larger than 1 and is larger for smaller values of f . We will show in the following that the spectral index of the upward-scattered photons, α_{up} , is systematically flatter than the angle-averaged one computed above. Good agreement with the observed “universal” value of $\alpha = 0.9$ (e.g., Pounds et al. 1990) can be reached, however, only for values of f close to 1.

The blackbody temperature was fixed at $kT_{BB} = 50$ eV. The dependence of the results on this value is small: for kT_{BB} varying between 5 and 500 eV, the change in α is less than 0.1.

For low τ the temperature reaches values close to mc^2 , at which production of electron-positron pairs may become important.

3. ROLE OF PAIR PRODUCTION

From the theory of thermal plasmas in pair equilibrium (Svensson 1984; Zdziarski 1985) the pair density can be computed for a given value of T_C and τ_p , where τ_p is the optical depth of the corona in the absence of pairs. As a result, the total optical depth of the corona will be given by $\tau = \tau_p + \tau_{e^+e^-}$.

The contribution of pairs depends on the compactness parameter, l_c , which for a two-phase disk system of radius R and vertical thickness H for the hot phase, releasing a total luminosity L , can be defined as follows:

$$l_c = \frac{\sigma_T}{m_e c^3} \frac{H}{R^2} L \sim 10^4 \times \frac{h}{r^2} \frac{L}{L_{\text{Edd}}}, \quad (8)$$

where r and h are expressed in units of gravitational radii $2GM/c^2$, and L_{Edd} is the Eddington luminosity. The pair balance equation can be written synthetically in the form

$$\tau_p^2 = \tau^2(1 - \Lambda), \quad (9a)$$

where

$$\Lambda = \left(\frac{N_p}{n_e}\right)^2 \left[f_{PP} + \frac{N_W}{N_p} f_{PW} + \left(\frac{N_W}{N_p}\right)^2 f_{WW} \right] / f_A. \quad (9b)$$

Here n_e is the number density of electrons and positrons and N_W and N_p are related to the densities of photons in the Wien and power-law portion of the spectrum, respectively. The terms f_{PP} , f_{PW} , f_{WW} are dimensionless pair production rates from photon-photon interaction where the photons belong to the power law (P) and Wien (W) portion of the spectrum, while f_A is the annihilation rate. All these terms are precisely defined in Svensson (1984) and Zdziarski (1985). In writing equation (9b) no pair escape is allowed beside annihilation.

It is important to recall that the energy balance equations determine T_C and α consistently with a given value of the total optical depth τ , irrespectively of τ_p and l_c . For fixed l_c , equations (9a) and (9b) yield then the value of τ_p consistent with τ , T_C , and α satisfying the balance equations. The solution of equation (7) coupled with equations (9a) and (9b) for the total optical depth τ is shown in Figure 2, with τ_p as parameter and l_c as the independent variable. For low l_c pairs are not important and $\tau = \tau_p$. For high l_c , a solution $\{\tau, T_C, \alpha\}$ corresponds to a value of τ_p lower than τ . As pointed out by Svensson (1984), for given compactness, the maximum temperature is obtained for the minimum total optical depth, that is for a pure pair plasma, $\tau_p = 0$. In this limit equation (9a) reduces to $\Lambda(l_c, \tau, T_C, \alpha) = 1$, which yields an upper limit to the temperature and a lower limit to the total optical depth τ .

For high values of l_c (10^2 – 10^4), the total depth is between 0.1 and 1 as shown in Figure 2, irrespectively of the value of τ_p . In this range of compactness, the maximum temperature is 250–70 keV. Lower values of l_c allow higher values of the temperature and lower values of the optical depth. Note that for a given value of the source luminosity, because of the geometrical factor h/r in expression (8), the compactness is lower for a slablike geometry than for a spherical one.

4. REALISTIC EMISSION SPECTRA

The quasi-analytic approximations used above have been necessary in order to derive approximate spectral properties which in turn allowed us to determine the physical parameters of the Comptonization region in a consistent way. Once these

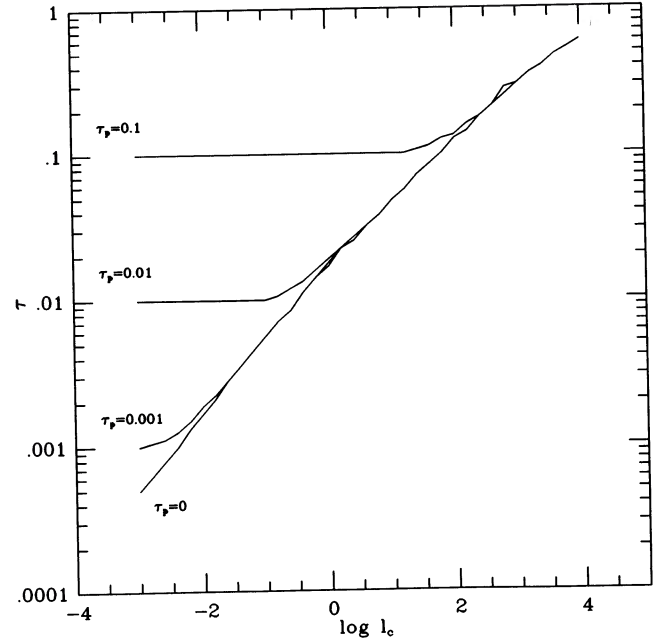


FIG. 2.—Total optical depth τ as a function of compactness parameter l_c and original electron optical depth τ_p . The limiting curve is for a pure pair corona. The corresponding coronal temperature can be read from Fig. 1.

parameters have been derived, one can perform Monte Carlo simulations (see Pozdynakov et al. 1983) to produce more realistic emission spectra.

We consider a photon source on one side of the slab, with a blackbody spectrum at $kT_{\text{BB}} = 50$ eV and determine separately the energy distributions of photons emerging from the two sides of the slab: the side opposite to that of incidence (transmitted photons) and the same side (backscattered photons).

The spectra of transmitted and backscattered photons differ significantly in shape in the energy range corresponding to the first scattering, which is clearly due to the higher probability and energy transfer of head on collisions: the transmitted component is flatter and contains slightly less power than the backscattered one (Fig. 3). In order to characterize the spectral shape, we performed power-law best fits of the Monte Carlo distributions in the 2–30 keV range. The results are reported in Table 1 as α_{up} , together with the average value derived in § 2, for various values of τ .

In a second step we compute the integrated albedo and the energy distribution of the “reflected” photons. The sum of the transmitted and reflected components which build up the emitted spectrum is shown in Figure 3. Spectral indices for the “observed” energy distribution, estimated by best fits in the 2–30 keV range, are also reported in Table 1. The ratio between the total UV and X-ray luminosities is ~ 1 , determined by f only, and is about 3 if the X-ray luminosity is computed in the (2–30) keV range, for $\tau = 0.1$. The ratio increases with decreasing τ and depends on the actual viewing angle.

Finally we estimate the equivalent width of the Fe line for an isotropic distribution of downscattered ionizing photons and assuming that photoionization of the $K\alpha$ level occurs at an effective optical depth ~ 1 . The effective optical depth is

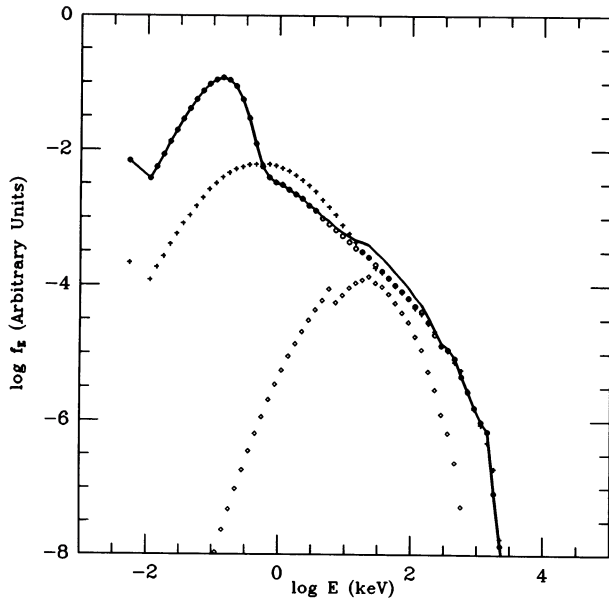


FIG. 3.—Monte Carlo simulation of the emitted spectrum (solid line), obtained adding the upward Comptonized spectrum (open circles) and the reflected component (diamonds). The downward Comptonized spectrum (crosses) is also shown. The hot phase parameters are $\tau = 0.1$, $\Theta = 0.51$. The soft photon source is a blackbody with $kT = 50$ eV.

defined as in Rybicki & Lightman (1979), considering the opacity of the thick layer as due to iron bound-free absorption and electron scattering. The results are reported in Table 1. Due to the enhanced flux of backscattered photons with respect to the transmitted ones, the equivalent width can be somewhat in excess of the usual 2π case. A clear prediction of the present model is that the line will be broadened by electron scattering in the hot layer.

5. DISCUSSION AND CONCLUSION

The main new aspect of the model is the treatment of the coupling of the two phases. If energy dissipation occurs mainly in the hot phase, i.e., $f \approx 1$, the three components observed in the X-ray spectra of Seyfert galaxies can be understood. The shape of the power-law component and its small dispersion are accounted for and the strength of the reflection bump and of the Fe line are explained due to the 2π solid angle and to the

TABLE 1
RESULTS OF POWER-LAW FITS

τ_{es}	Θ	EW ^a ($i = 0^\circ$) (eV)	α_{av} ^b	α_{up} ^c	$\alpha_{up+refl}$ ^d	$(A-1)_{MC}$ ^e
0.03.....	1.	350	1.2	0.85	0.65	1.9
0.05.....	0.76	300	1.25	0.9	0.7	2.0
0.1.....	0.51	250	1.25	0.85	0.7	2.2
0.25.....	0.28	160	1.3	1	0.85	2.3
0.5.....	0.16	140	1.35	1.1	0.9	2.1

^a Iron line equivalent width expected for a disk seen almost face-on.

^b "Average" spectral index derived from the balance equations for $f = 1$.

^c Spectral index derived from the best fit of the Monte-Carlo simulations of the upward Comptonized component in the (2–30) keV range.

^d Spectral index derived from the best fit of the Monte Carlo simulations of the sum of the upward Comptonized component plus the reflected one in the (2–30) keV range.

^e Compton amplification factor derived from integration of Monte Carlo spectra. The analytical value for $f = 1$ is $A = 2$.

backward asymmetry of the Comptonized flux. Obviously, additional contributions to the reflection bump and to the Fe line may come from cold material further out.

A model along similar lines, in the context of explaining the X-ray and γ -ray background by AGNs, is being proposed by Field & Rogers (1991), who considered nonthermal particle acceleration in a magnetic corona. A consistent solution for a two-temperature layer, in principle similar to ours, was found by analytic methods for $\tau > 1$ by Sunyaev & Titarchuk (1989) in the case of neutron star accretion.

The model is tightly constrained: in order to reproduce the average slope observed in Seyfert galaxy spectra in the medium X-ray range, it is required that practically all the power be dissipated directly within the hot layer. It is possible to relax this requirement introducing a covering factor of the hot phase with respect to the thick one. Part of the blackbody luminosity would then emerge freely and the soft photon flux available for Comptonization would be smaller, allowing larger values of the amplification and flatter spectra.

A prediction testable by the presently operating γ -ray observatories (*GRO*, *GRANAT*) is the presence of a thermal cutoff between 200 keV and 2 MeV for sources with $10^4 > l_c > 1$. The expected correlation of L_s and L_{uc} is complex, depending on whether variability is due to changes in P_G or f or τ , and will be deferred to a future paper.

REFERENCES

- Begelman, M. C., & de Kool, M. 1990, in *Structure and Emission Properties of Accretion Disks*, ed. C. Bertout, S. Collin, J. Plasota, & J. Tran Than Van (Gif sur Yvette: Editions Frontières), 143
- Burm, H. 1986, *A&A*, 165, 220
- Field, G. B., & Rogers, R. D. 1991, in *Proc. Heidelberg Conf. on the Physics of AGNs*, in press
- Guilbert, P. W. & Rees, M. J. 1988, *MNRAS*, 233, 475
- Heyvaerts, J. 1990, in *Structure and Emission Properties of Accretion Disks*, ed. C. Bertout, S. Collin, J. Plasota, & J. Tran Than Van (Gif sur Yvette: Editions Frontières), 109
- Katz, J. I. 1976 *ApJ*, 206, 910
- Kunieda, H., Turner, T. J., Awaki, H., Koyama, K., Mushotzky, R. F., & Tsusaka, Y. 1990, *Nature*, 345, 786
- Lightman, A. P., & White, T. R. 1988, *ApJ*, 335, 57
- Maraschi, L., Roasio, R., & Treves, A. 1982, *ApJ*, 253, 312
- Mushotzky, R. F. 1984, *Adv. Space Res.*, 3(10–12), 157
- Pounds, K. A., Nandra, K., Stewart, G. C., George, I. M., & Fabian, A. C. 1990, *Nature*, 344, 132
- Pozdnyakov, L. A., Sobol, I. M., & Sunyaev, R. A. 1976, *Sov. Astron. Lett.*, 2, 55
- . 1983, in *Sov. Sci. Rev./Sec. E: Astr. Space Phys. Rev.*, Vol. 2, ed. R. A. Sunyaev (New York: Harwood), 189
- Rothschild, R. E., Mushotzky, R. F., Baity, W. A., Gruber, D. E., Matteson, J. L., & Peterson, L. E. 1983, *ApJ*, 269, 423
- Rybicki, G. B., & Lightman, A. P. 1979, *Radiative Process in Astrophysics* (New York: Wiley)
- Shapiro, S. L., Lightman, A. P., & Eardley, D. M. 1976, *ApJ*, 204, 187
- Sunyaev, R. A., & Titarchuk, L. G. 1980, *A&A*, 86, 121
- . 1989, in *Proc. of the 23rd ESLAB Symp.*, ed. J. Hunt & B. Batrick (ESA SP-286) (Noordwijk: ESA), 627
- Svensson, R., 1984, *MNRAS*, 209, 175
- Takahara, F., Tsuruta, S., & Ichimaru, S. 1981, *ApJ*, 251, 26
- Turner, T. J., & Pounds, K. A. 1989, *MNRAS*, 240, 833
- Zdziarski, A. A. 1985, *ApJ*, 289, 514
- Zdziarski, A. A., Ghisellini, G., George, I. M., Fabian, A. C., Svensson, R., & Done, C. 1990, *ApJ*, 363, L1